BULLETIN OF THE POLISH ACADEMY OF SCIENCES
TECHNICAL SCIENCES, Vol. 61, No. 4, 2013
DOI: 10.2478/bpasts-2013-0086

Dedicated to Professor M.P. Kaźmierkowski
on the occasion of his 70th birthday

Unscented and extended Kalman filters study for sensorless control of PM synchronous motors with load torque estimation

K. ZAWIRSKI, D. JANISZEWSKI*, and R. MUSZYNSKI

Poznan University of Technology, 3a Piotrowo St., 60-965 Poznań, Poland

Abstract. This paper describes a study and the experimental verification of sensorless control of permanent magnet synchronous motors using Kalman filters. There are proposed two structures, extended and unscented Kalman filters, which use only the measurement of the motor current for on-line estimation of speed, rotor position and load torque reconstruction. The Kalman filter is an optimal state estimator and is usually applied to a dynamic system that involves a random noise environment. These structures are described in detail, starting with the selection of the variables state vector, the filters structure, and ending with in-depth laboratory tests. It has become possible, without using position and torque sensors, to apply these control structures as a cost-effective solution. Experimental results confirm the validity of the proposed estimation techniques.

Key words: Kalman filters, control system synthesis, machine vector control, sensorless drives, velocity control, permanent magnet synchronous motor.

1. Introduction

Permanent magnet synchronous motor drives [1–31] are widely used in industrial processes, due to their inherent high torque to inertia ratio (high flux density), small size and enhanced dynamic performance [1, 14, 21]. Field oriented control (FOC) allows obtaining the maximum performance but requires information about the shaft position [13, 30]. The effects of a sensorless FOC of a PMSM depend strongly on the quality of estimation of the state variables and disturbances.

Systems called sensorless have the potential to get rid of any mechanical sensors placed on the machine shaft, usually for position and velocity measurements. This paper presents some extension of the state vector by adding to it a load torque, which is estimated. There is a current work on several methods to find the status of the propulsion system based on measurement of readily available drive terminal variables [2, 4, 5, 7, 11, 15, 17, 22, 24, 30]. These methods are called observers. One of them is the Kalman filter, based on mathematical dependencies formulated by Rudolf Kalman [12]. The observers use only direct signals – stator voltages, as well as variables measuring terminal – phase stator currents. Several method have been developed in order to obtain mechanical quantities of PMSM which can be used for sensorless control [3, 6–8, 20, 23, 29, 31].

The proposed playback system allows estimating the state, all variables occurring in the classical mathematical model of synchronous motor with permanent magnet and the torque load brought into the effects on the motor shaft, which is often treated as a disturbance [6–8, 19, 28].

This paper is organised as follows. First, the design considerations are presented, and some problems in sensorless control with an extended estimated state vector is indicated. Next the model of the PMSM is proposed. Then, the theoretical background of Extended and Unscented Kalman filters is presented. Finally, the effectiveness of the proposed sensorless control system is verified by experiments.

2. Design considerations

2.1. Sensorless control. Sensorless control is based on eliminating the necessity of using a shaft angular position transducers, in a broad perspective, to eliminate any mechanical sensors placed on the machine shaft. Elimination of mechanical sensors provides advantages such as: increased reliability of the drive, the ability to work in adverse environmental conditions, and a decrease in the cost of the drive [8, 13, 30].

Field oriented control is a versatile method of controlling the PMSM, where the field oriented theory is used to control space vectors of the magnetic flux, current, and voltage [16, 18, 30]. The control scheme is relatively simple (Fig. 1), the excitation flux from permanent magnets is frozen to the direct d axis of the rotor and thus its position can be obtained directly from the rotor shaft by measuring the rotor angle. An optimally efficient operation is achieved by stator current control which ensures that the stator current phasor contains only a quadrature q axis component by the PWM voltage converter [13, 18]. It is possible to set up the co-ordinate system to decompose the vectors into how much electromagnetic field is generated and how much torque is produced [14]. This control technique guarantees a good dynamic performance of PMSM.

*e-mail: dariusz.janiszewski@put.poznan.pl

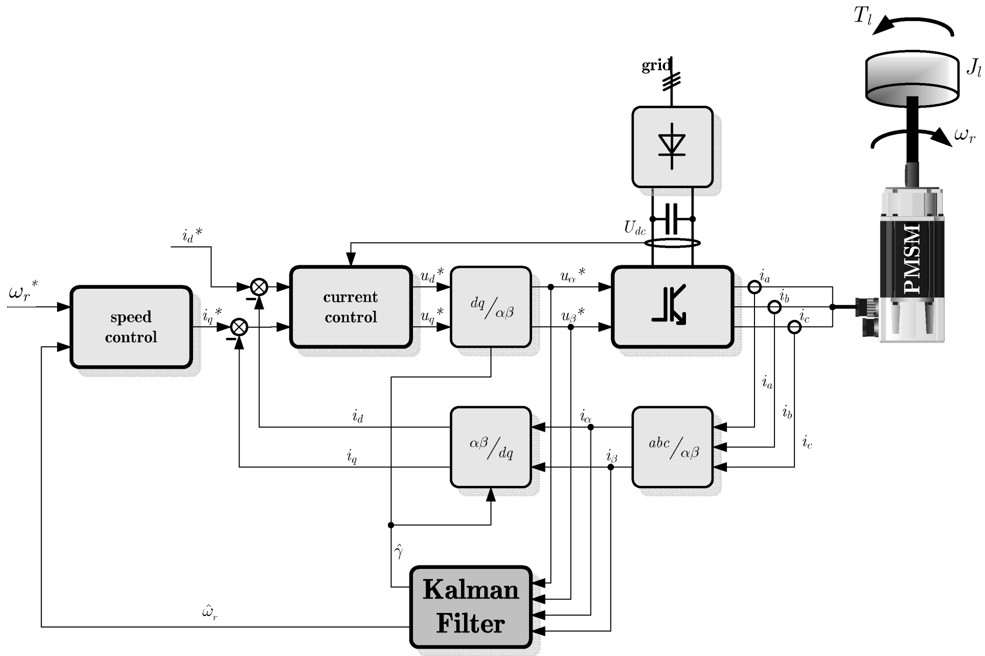

Fig. 1. The proposed sensorless drive

2.2. Estimation vector. Some state variables are necessary during estimation because they are an important part of a state space model. Additional novel estimated variables such as the load torque T_l can be added. Their value can be helpful during the control of the complex mechanical structures of drives. The problem of observing which has often been noted in the literature [3, 27, 31]. It is interesting to extend a observation vector to the load torque. So the estimation of the state space vector of the proposed observer is:

$$\underline{\widehat{x}} = \begin{bmatrix} i_d & i_q & \omega_r & \gamma & T_l \end{bmatrix}^T, \tag{1}$$

where: i_d and i_q are the dq axis currents, ω_r is mechanical speed,γ is electrical shaft position and T_l is occurred load torque.

2.3. Mathematical model of motor directed into observer The mathematical model of a PMSM has three main parts: the electrical network, the electromechanical torque production, and the mechanical subsystem [21]. The stators of a PMSM and an IM are similar. The rotor consists of permanent magnets, there are modern rare-earth magnets with high strength of the magnetic field.

In the mathematical model, during examining the problem, some simplifications are made: saturation is neglected, induced electromagnetic force is sinusoidal, eddy currents and hysteresis losses are neglected, no dynamical dependencies in air-gap, no rotor cage. With these assumptions, the rotor oriented dq electrical network equations of PMSM can be described as:

$$u_d = R_s i_d + L_d \frac{di_d}{dt} - p\omega_r L_q i_q, \tag{2}$$

$$u_q = R_s i_q + L_q \frac{di_q}{dt} + p\omega_r L_d i_d + p\omega_r \Psi_m. \tag{3}$$

where u_d and u_q are the dq axis voltages, L_d and L_q are the dq axis inductances, R_s is the stator resistance, and Ψ_m is the flux produced by the permanent magnets on the rotor.

The electric torque is

$$T_e = \frac{3}{2} \cdot p \left[\Psi_m - (L_q - L_d)\, i_d\right] \cdot i_q, \tag{4}$$

where p is the number of pole pairs, and $\frac{3}{2}$ stems from frame conversion: perpendicular stator $\alpha\beta$ into rotor dq.

The drive dynamics can be described as

$$T_e - T_l = J\frac{d\omega_r}{dt}, \tag{5}$$

where T_l is the load torque and J is the summary moment of inertia of the kinematic chain.

Based on (4) and (5), the movement equation can be written:

$$\frac{d\omega_r}{dt} = \frac{p}{J}\left[\frac{3}{2}\left(\Psi_m - (L_q - L_d)\, i_d\right) \cdot i_q\right] - \frac{T_l}{J}. \tag{6}$$

The position γ can be described by a differential equation:

$$\frac{d\gamma}{dt} = p \cdot \omega_r. \tag{7}$$

Many speed observers described in the literature do not recognise load torque [4, 30]. In these observers, the velocity is assumed to be constant over short periods of time and the load torque is treated as an unknown disturbance that is not observed. In this work the load torque was introduced to the state vector and can be estimated only with assumption, the load torque T_l is invariable in a narrow interval:

$$\frac{d}{dt}T_l \approx 0. \tag{8}$$

This is the main assumption in the work.

The state space model can be described classically as

$$\underline{\widehat{x}}_k = \mathbf{F}_k(\underline{\widehat{x}}_{k-1})\underline{\widehat{x}}_{k-1} + \mathbf{B}_k(\underline{\widehat{x}}_{k-1})\underline{u}_k, \tag{9}$$

$$\underline{z}_k = \mathbf{H}_k(\underline{\widehat{x}}_k)\underline{\widehat{x}}_k, \tag{10}$$

The system matrix $\mathbf{F}_k$ is

$$\mathbf{F}_k(\underline{\widehat{x}}_k) = \begin{bmatrix} 1 - T_s \cdot \dfrac{R_s}{L_d} & T_s \cdot \omega_r \dfrac{L_q}{L_d} & 0 & 0 & 0 \\ -T_s \cdot \omega_r \dfrac{L_d}{L_q} & 1 - T_s \cdot \dfrac{R_s}{L_q} & -T_s \cdot \dfrac{\Psi_m}{L_q} & 0 & 0 \\ 0 & T_1 & 0 & 0 & -T_s \cdot \dfrac{1}{J} \\ 0 & 0 & T_s & 1 & 0 \\ 0 & 0 & 0 & 0 & 1 \end{bmatrix}, \tag{11}$$

where

$$T_1 = T_s \cdot \frac{3}{2}\frac{p}{J}\left[\Psi_f - (L_q - L_d)\, i_d\right]$$

The output matrix $\mathbf{H}_k$ is

$$\mathbf{H}_k(\underline{\widehat{x}}_k) = \begin{bmatrix} \cos\gamma & -\sin\gamma & 0 & 0 \\ \sin\gamma & \cos\gamma & 0 & 0 \end{bmatrix}, \tag{12}$$

and the matrix $\mathbf{B}_k$

$$\mathbf{B}_k(\underline{\widehat{x}}_k) = \begin{bmatrix} T_s \cdot \dfrac{1}{L_d}\cos\gamma & T_s \cdot \dfrac{1}{L_d}\sin\gamma \\ -T_s \cdot \dfrac{1}{L_q}\sin\gamma & T_s \cdot \dfrac{1}{L_q}\cos\gamma \\ 0 & 0 \\ 0 & 0 \\ 0 & 0 \end{bmatrix}. \tag{13}$$

3. The Kalman filter

By definition, the Kalman filter is a recursive filter with infinite impulse response [12]. This means that the derivative of the known estimate $\frac{d}{dt}\underline{x}$, called the trend, actual output measure $\underline{y}_k$ are sufficient to calculate the estimate of the current state of the system $\underline{x}_k$ at each time $t\epsilon(0,\infty)$. For the Kalman filter it is not necessary to know the history of observations. Kalman filter states can be described by two variables: $\frac{d}{dt}\underline{x}$ – derivative of the current state estimate obtained based on knowledge of observation and $\mathbf{P}_{k|k}$ – error covariance matrix (uncertainty of observation) estimation process.

The Kalman filter estimation process is divided into two separate stages which are cyclical: *prediction* and *correction*. The whole process of calculating the filter is performed recursively to obtain the optimum value of the corrector $\mathbf{K}_k$ with the assumed error ε. A prediction is used to determine the state estimate $\underline{\widehat{x}}$ based on the trend and input signal $\underline{u}$. Correction, however, leads to improvements in the new estimate of the exact value $\underline{\widehat{x}}$ based on the measured output $\underline{y}_k$ and the value of the corrector $\mathbf{K}_k$.

Prediction. This is also called time actualisation, and is based on knowing the derivative of the state $\frac{d}{dt}\underline{\widehat{x}}$. It is described as a dependency in the presence of input $\underline{u}$. It can be served as an expression:

$$\frac{d}{dt}\underline{\widehat{x}} = \mathbf{F}_k\underline{\widehat{x}} + \mathbf{B}_k\underline{u}. \tag{14}$$

Filtering at this stage, it is assumed also update with a vector of state variables $\underline{x}$ of the system covariance $\mathbf{P}$, based on state function (14):

$$\mathbf{P}_{k|k-1} = \mathbf{F}_k\mathbf{P}_{k-1|k-1}\mathbf{F}_k^{\mathrm{T}} + \mathbf{Q}. \tag{15}$$

Correction. Correction, which is the actualisation of the measurement, involves the introduction of the correction signal based on the measured output $\underline{z}_k$. It is defined as the difference in response values of the observer and the measured output signal, like a residual:

$$\underline{\tilde{y}}_k = \underline{z}_k - \mathbf{H}_k\underline{\widehat{x}}_{k|k-1}. \tag{16}$$

Additionally, there is introduced, based on knowledge of the measurement covariance $\mathbf{R}$, the innovation covariance system:

$$\mathbf{S}_k = \mathbf{H}_k\mathbf{P}_{k|k-1}\mathbf{H}_k^{\mathrm{T}} + \mathbf{R}. \tag{17}$$

Based on the above, the corrector can be determined by

$$\mathbf{K}_k = \mathbf{P}_{k|k-1}\mathbf{H}_k^{\mathrm{T}}\mathbf{S}_k^{-1}, \tag{18}$$

which together with the calculated value of the residual (16) corrects the state vector:

$$\underline{\widehat{x}}_k = \underline{\widehat{x}}_{k-1} + \mathbf{K}_k\underline{\tilde{y}}_k. \tag{19}$$

With this correction of the state vector $\underline{\widehat{x}}_k$, the covariance is also corrected:

$$\mathbf{P}_{k|k} = (I - \mathbf{K}_k\mathbf{H}_k)\mathbf{P}_{k|k-1}. \tag{20}$$

The above formula for the Kalman filter is valid only for linear systems and optimal Kalman gain $\mathbf{K}_k$ [12]. Based on the above assumptions, $\mathbf{P}_{k|k}$ and the Kalman gain $\mathbf{K}_k$ are constant, and can be computed once based on constant $\mathbf{F}_k$, $\mathbf{B}_k$, $\mathbf{H}_k$. The calculation is usually carried out by this procedure iteratively until there is a certain convergence to a consistent result.

There are many developments of the procedure gain $\mathbf{K}_k$ calculations which reduce the computational complexity. There are *extended Kalman filters* and *unscented Kalman filters*, both for nonlinear systems, described below.

3.1. Extended Kalman filter.

The extended Kalman filter (EKF) is de facto an extension of the classical Kalman filter to the area of nonlinear objects. The calculations are performed periodically, and data from the previous step are used to calculate and predict the current step, which in turn predicts the next step. So the whole algorithm described below is recurrent. The main extension is to introduce a nonlinear state function $\mathbf{F}$ as $f(\underline{x}_{k-1}, \underline{u}_k))$ and output function $\mathbf{H}$ as $h(\underline{x}_k)$ of mathematical model of the object based on the actual state $\underline{x}_k$ and input $\underline{u}_k$:

$$\underline{x}_k = f(\underline{x}_{k-1}, \underline{u}_k) + \underline{w}_k, \tag{21}$$

$$\underline{z}_k = h(\underline{x}_k) + \underline{v}_k. \tag{22}$$

As can be seen by analysing the classical Kalman filter, functions f and h cannot be used in a natural form or as a differential. The solution may be applied to the Jacobians in the working point of state vector $\underline{x}_k$ and input $\underline{u}_k$.

In the analysis of the EKF it is necessary to calculate the Jacobian matrix of the discretized state f and output h functions. This process takes the linearisation of nonlinear functions in the neighborhood of the working point $\widehat{\underline{x}}_{k|k-1}$ where the state transition Φ_k and output $\mathbf{h}_k$ matrices are defined to be the following:

$$\Phi_k = \left.\frac{\partial f}{\partial \underline{x}}\right|_{\widehat{\underline{x}}_{k-1|k-1},\underline{u}_k}, \tag{23}$$

$$\mathbf{h}_k = \left.\frac{\partial h}{\partial \underline{x}}\right|_{\widehat{\underline{x}}_{k|k-1}}. \tag{24}$$

It should be noted that Jacobians should be counted in each step k of prediction. The built up matrices Φ_k i $\mathbf{h}_k$ can be used in prediction and correction equations.

Prediction. Prediction is based on the dependency of the classical Kalman filter but including Jacobians. For state prediction (14) one has

$$\widehat{\underline{x}}_{k|k-1} = f(\widehat{\underline{x}}_{k-1|k-1}, \underline{u}_k), \tag{25}$$

and for the covariances (15),

$$\mathbf{P}_{k|k-1} = \Phi_k \mathbf{P}_{k-1|k-1} \Phi_k^T + \mathbf{Q}_k. \tag{26}$$

Correction. The correction in the EKF is based on classical correction having regard to Jacobians. The residual (16) is now

$$\tilde{\underline{y}}_k = \underline{z}_k - h(\widehat{\underline{x}}_{k|k-1}), \tag{27}$$

covariance (17) is:

$$\mathbf{S}_k = \mathbf{h}_k \mathbf{P}_{k|k-1} \mathbf{h}_k^T + \mathbf{R}_k. \tag{28}$$

Based on above equation and defined Jacobian $\mathbf{h}_k$ can reach the optimal Kalman gain:

$$\mathbf{K}_k = \mathbf{P}_{k|k-1} \mathbf{h}_k^T \mathbf{S}_k^{-1}. \tag{29}$$

The correction is performed as in (19):

$$\widehat{\underline{x}}_{k|k} = \widehat{\underline{x}}_{k|k-1} + \mathbf{K}_k \tilde{\underline{y}}_k. \tag{30}$$

A simplified form for the correction of the covariance $\mathbf{P}_{k|k}$ is

$$\mathbf{P}_{k|k} = (I - \mathbf{K}_k \mathbf{h}_k) \mathbf{P}_{k|k-1}. \tag{31}$$

3.2. Unscented Kalman filter. The main problem with the estimation of nonlinear systems is that it is difficult to determine the probability distribution, nonlinear function of state and output [9, 10, 25, 26]. It appears that the nonlinear transformation of the deviation and *Jacobians* needed for an EKF does not determine the real covariances. An EKF is based on the classical Kalman filter assumptions about the linearity of the object and it is in this way that the covariances are calculated [12, 25]. For nonlinear objects, covariances are associated with the process, but can not be linked to linearised models of the object. Based on the particular analysis of nonlinear systems where the covariance of the state should not be associated with a linearised system, and can even be far from them.

An Unscented Kalman filter is an improvement over the EKF algorithm. S. Julier and J. Uhlman proposed in [9] a completely novel solution of the estimation theory problem based on *unscented transformations*. These authors found it easier to approximate the Gaussian distribution associated with each state vector variable, rather than approximate the nonlinear transformation function. This made it possible to simplify the algorithm by eliminating the need for calculating the Jacobians. This is based on two assumptions: the first is the determination of the non-linear transform of the function at work, and not in the whole range of the probability density distribution function. The second point concerns the search for work in which this density corresponds to the actual decomposition of the nonlinear system. This filter, like its classical form, is based on two cycles of procedures: prediction and correction.

Prediction. Prediction can be used independently the UKF update, in combination with a linear update. As assumed in the classical Kalman filter approach, and as it is the case for extended filter prediction, one proceeds in a similar way for each solution. In this case, however, the extend estimation state vector of the value of disturbances. Such a procedure makes it possible to estimate the state vector and its environment. Strictly, this surround will transform non-linear disturbances [9].

A new $\underline{x}^a_{k-1|k-1}$ vector is defined:

$$\underline{x}^a_{k-1|k-1} = [\widehat{\underline{x}}^T_{k-1|k-1} \quad E\langle \underline{w}_k^T\rangle \quad E\langle \underline{v}_k^T\rangle\ ]^T. \tag{32}$$

So it is natural to define its covariances, which are formed by taking the covariances of the state vector $\mathbf{P}_{k-1|k-1}$, the known process noise covariance $\mathbf{Q}_k$, and the distortion measurement $\mathbf{R}_k$. It therefore assumes the form

$$\mathbf{P}^a_{k-1|k-1} = \begin{bmatrix} \mathbf{P}_{k-1|k-1} & 0 & 0 \\ 0 & \mathbf{Q}_k & 0 \\ 0 & 0 & \mathbf{R}_k \end{bmatrix}. \tag{33}$$

A set of $2L+1$ sigma points, $\chi_{k-1|k-1}$, is derived from the augmented state and covariance where L is the dimension of the augmented state:

$$\chi^0_{k-1|k-1} = \underline{x}^a_{k-1|k-1}, \tag{34}$$

$$\chi^i_{k-1|k-1} = \underline{x}^a_{k-1|k-1} + \left(\sqrt{(L+\lambda)\mathbf{P}^a_{k-1|k-1}}\right)_i, \quad \text{for } i = 1..L, \tag{35}$$

$$\chi^i_{k-1|k-1} = \underline{x}^a_{k-1|k-1} - \left(\sqrt{(L+\lambda)\mathbf{P}^a_{k-1|k-1}}\right)_{i-L}, \quad \text{for } i = L+1, \ldots 2L, \tag{36}$$

The matrix square root $\left(\sqrt{n\mathbf{P}_k}\right)$ should be calculated using numerically efficient and stable methods such as the

Cholesky decomposition. The sigma points $\chi^i_{k|k-1}$ are propagated through the state space transition function (14):

$$\chi^i_{k|k-1} = \mathbf{F}_k \chi^i_{k-1|k-1} + \mathbf{B}_k \underline{u}_k, \quad i = 0..2L. \tag{37}$$

The weighted sigma points $\chi^i_{k|k-1}$ are recombined to produce the predicted state $\widehat{\underline{x}}_{k|k-1}$ and covariance $\mathbf{P}_{k|k-1}$:

$$\widehat{\underline{x}}_{k|k-1} = \sum_{i=0}^{2L} W^i_s \chi^i_{k|k-1}, \tag{38}$$

$$\mathbf{P}_{k|k-1} = \sum_{i=0}^{2L} W^i_c \, [\chi^i_{k|k-1} - \widehat{\underline{x}}_{k|k-1}][\chi^i_{k|k-1} - \widehat{\underline{x}}_{k|k-1}]^T, \tag{39}$$

where the weights W_s and W_c for the state and covariance are given by

$$W^0_s = \frac{\lambda}{L+\lambda}, \tag{40}$$

$$W^0_c = \frac{\lambda}{L+\lambda} + (1 - \alpha^2 + \beta), \tag{41}$$

$$W^i_s = W^i_c = \frac{1}{2(L+\lambda)}, \tag{42}$$

where α, β, κ are noise distribution parameters, and λ is chosen arbitrarily. They are helpful during filter tuning [10]. Typical values for α, β and κ for the majority of applications in which the disturbance is located in the Gaussian noise assumptions, are, respectively, 10^{-3}, 2 and 0. Any differences from these values can only lead to more easy tuning of the filter, because they add additional degrees of freedom.

Correction. Correction is adapted strictly from the classical form. The sigma points $\chi^i_{k|k-1}$ are projected through the observation function $\mathbf{H}_k$:

$$\Upsilon^i_k = \mathbf{H}_k \chi^i_{k|k-1}, \quad i = 0..2L. \tag{43}$$

Based on weight W^i_s and W^i_c from (42) and observation matrix Υ^i_k it is possible to obtain the output signal:

$$\widehat{\underline{z}}_k = \sum_{i=0}^{2L} W^i_s \Upsilon^i_k, \tag{44}$$

and also the output covariance:

$$\mathbf{P}_{z_k z_k} = \sum_{i=0}^{2L} W^i_c \, [\Upsilon^i_k - \widehat{\underline{z}}_k][\Upsilon^i_k - \widehat{\underline{z}}_k]^T. \tag{45}$$

The correction $\mathbf{K}_k$ depends directly on the state covariances $\mathbf{P}_{k|k-1}$ and innovation of system covariances $\mathbf{S}_k$, and so is similar to (45). Based on the Kalman correction definition,

$$K_k = \mathbf{P}_{x_k z_k} \mathbf{P}^{-1}_{z_k z_k}, \tag{46}$$

where $\mathbf{P}_{x_k z_k}$ is

$$\mathbf{P}_{x_k z_k} = \sum_{i=0}^{2L} W^i_c \, [\chi^i_{k|k-1} - \widehat{\underline{x}}_{k|k-1}][\gamma^i_k - \widehat{\underline{z}}_k]^T. \tag{47}$$

As in the classical Kalman filter, the output residual is

$$\underline{\tilde{y}}_k = \underline{z}_k - h(\widehat{\underline{x}}_{k|k-1}). \tag{48}$$

The correction of the state is done by

$$\widehat{\underline{x}}_{k|k} = \widehat{\underline{x}}_{k|k-1} + \mathbf{K}_k(\underline{z}_k - \widehat{\underline{z}}_k). \tag{49}$$

The adjusted covariance matrix $\mathbf{P}_{k|k}$ is a prediction of $\mathbf{P}_{k|k-1}$ corrected by weighted values:

$$\mathbf{P}_{k|k} = \mathbf{P}_{k|k-1} - \mathbf{K}_k \mathbf{P}_{z_k z_k} \mathbf{K}^T_k. \tag{50}$$

The algorithm is cyclic. Data from the actual step are the input data for the next.

4. Experimental results

For experimental verification of the proposed estimation method, a laboratory setup has been constructed. It consists of the surface mounted magnets PMSM, supplied from a three phase power IGBT inverter. The mechanical part of laboratory setup is presented in Fig. 2, consisting of two similar motors coupled by a stiff shaft. The load twin motor supplied from industrial controller. The voltage and currents signals are adjusted and sampled simultaneously with 12-bit A/D converters. The real rotor position is measured by a precision incremental encoder.

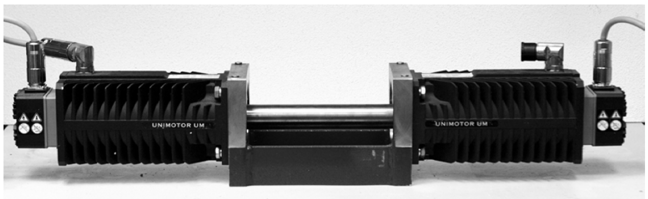

Fig. 2. Mechanical setup – twin PMSM with stiff shaft

This algorithm was implemented on an *Analog Devices Sharc 21369* Digital Signal Processor. The code has been mainly written in *C* language, except for low-level procedures in DPS Assembler. However the PWM generator was realised with additional *Altera Flex FPGA* used for independent fast hardware pulses generating. A real position is also computed using FPGA and sent to DSP by parallel memory fields. The execution time of the EKF and UKF algorithms is about 22 μs and 38 μs, respectively, while the control loop with acquisition takes 20 μs. The sampling time was chosen as $T_s = 100$ μs and it is the main superloop for current and speed control.

4.1. Extended Kalman filter

Speed demand. To test the behaviour of observers with a varying conditions of work it was decided to use tests involving a change of referenced speed ω^*_r. The first investigation was performed like a speed reference in stages: start, working set, reverse and braking. The maximum modulus of reference speed in this case was $\frac{1}{3}$ of maximum speed: $1000\frac{\text{rev}}{\text{min}} = 104.72\frac{\text{rad}}{\text{s}}$.

The results are presented in Fig. 3. Errors are plotted in detail in Fig. 4.

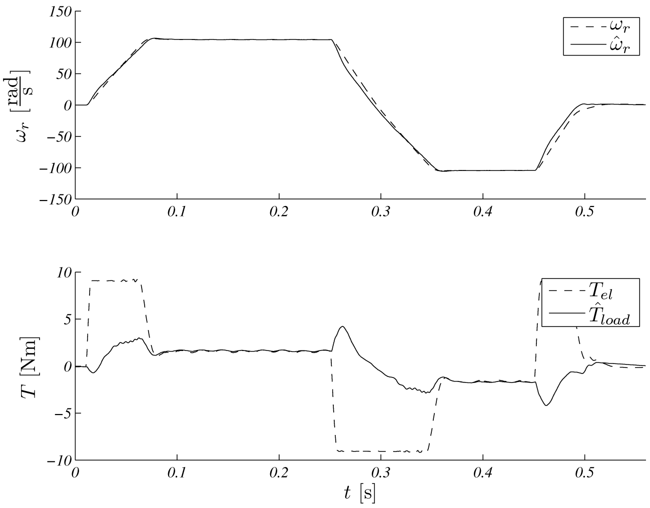

Fig. 3. EKF: reference speed $\omega_r^* = 104.72 \ \frac{\text{rad}}{\text{s}}$

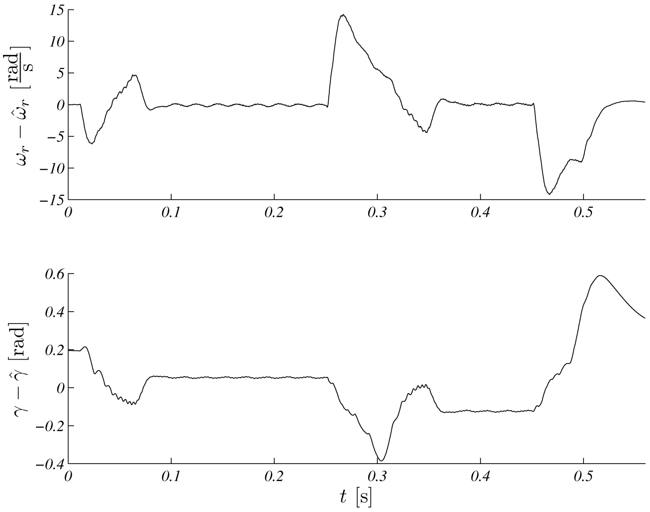

Fig. 4. EKF: reference speed $\omega_r^* = 104.72 \ \frac{\text{rad}}{\text{s}}$ – estimation errors

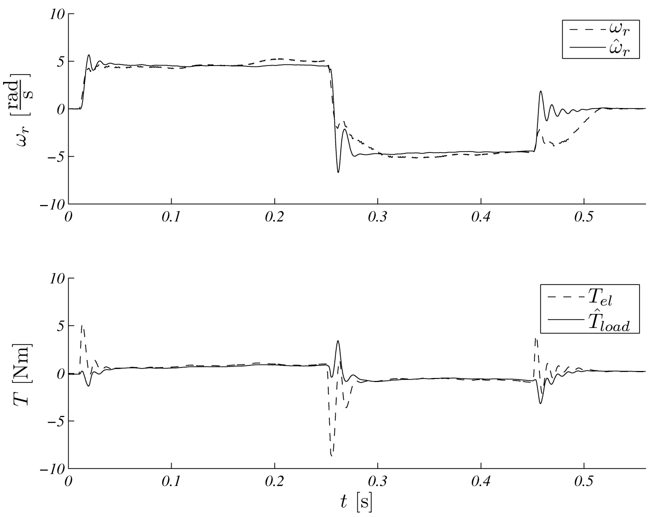

Fig. 5. EKF: reference speed $\omega_r^* = 5.28 \ \frac{\text{rad}}{\text{s}}$

A very interesting point of the works control system with an observer is the work during small speeds near zero. The same shape as above is presented in Fig. 5, but the maximum modulus is $\omega_r^* = 5.28 \ \frac{\text{rad}}{\text{s}}$. Experiment errors are presented in Fig. 6.

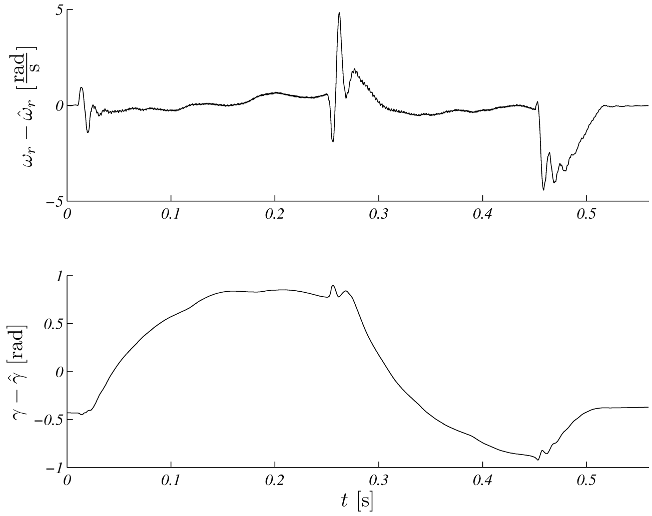

Fig. 6. EKF: reference speed $\omega_r^* = 5.28 \ \frac{\text{rad}}{\text{s}}$ – estimation errors

This type of a reference signal has significant stages for an observer behaviour such as: zero signal with no initial values in an estimation vector, and few steps of the demand speed.

Load torque. At this part of the investigation, the controlled system behaviour by the reference speed excitation and next stepped load torque was focussed on. This type of the reference signal has significant stages for its estimator behaviour such as: zero signal with no initial values in estimation vector, a step demand speed signal and an external load step. The constant reference speed is 104.72 rad/s and additional load torque is 3 Nm. A torque is applied and next removed. Results of the working are presented in Fig. 7, with errors in Fig. 8.

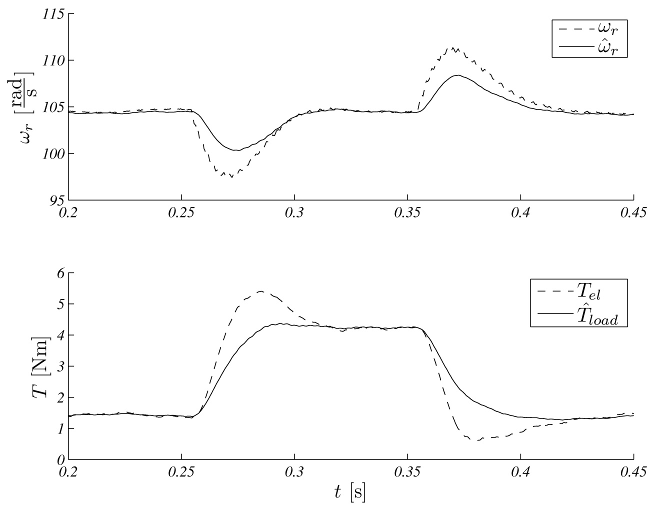

Fig. 7. EKF: load torque $T_l = 3\,\mathrm{Nm}$ response

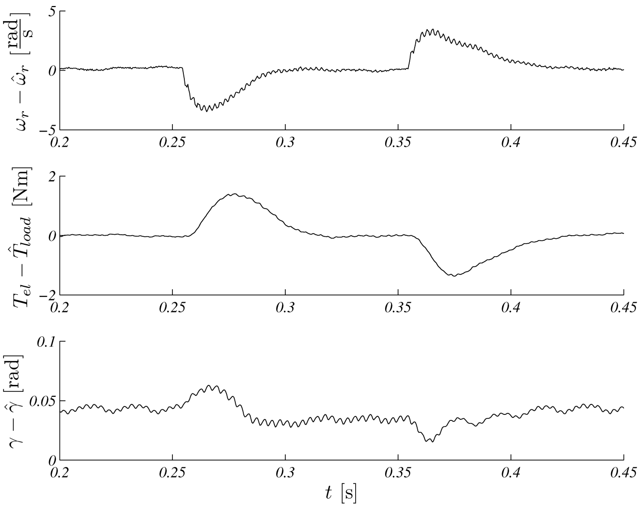

Fig. 8. EKF: load torque $T_l = 3\,\mathrm{Nm}$ response – estimation errors

This result shows good performance of the load torque estimation. In the case of a load torque variation, which was assumed nearly constant, it appears that the observer can cope with this problem at a level which is almost good.

4.2. Unscented Kalman filter

Speed demand. The idea of loading was presented in Subsec. "Speed demand". The results of working are presented in Fig. 9. Each investigation was performed in the same way.

The experimental results for low speed are presented in Fig. 11, and in Fig. 12 are the errors.

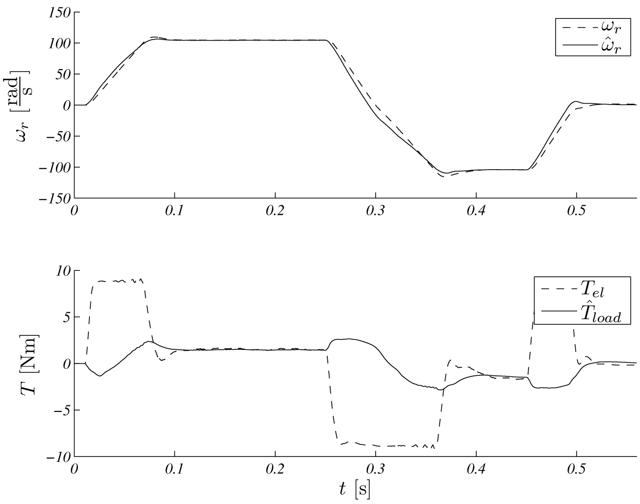

Fig. 9. UKF: reference speed $\omega_r^* = 104.72\ \frac{\mathrm{rad}}{\mathrm{s}}$

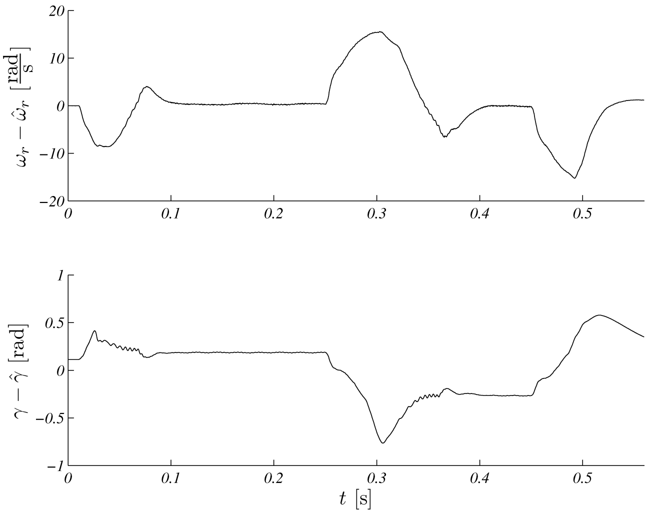

Fig. 10. UKF: reference speed $\omega_r^* = 104.72\ \frac{\mathrm{rad}}{\mathrm{s}}$ – estimation errors

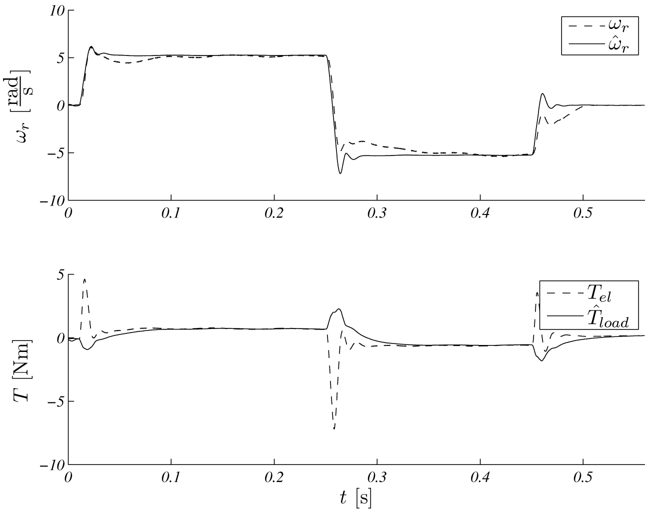

Fig. 11. UKF: reference speed $\omega_r^* = 5.28\ \frac{\mathrm{rad}}{\mathrm{s}}$

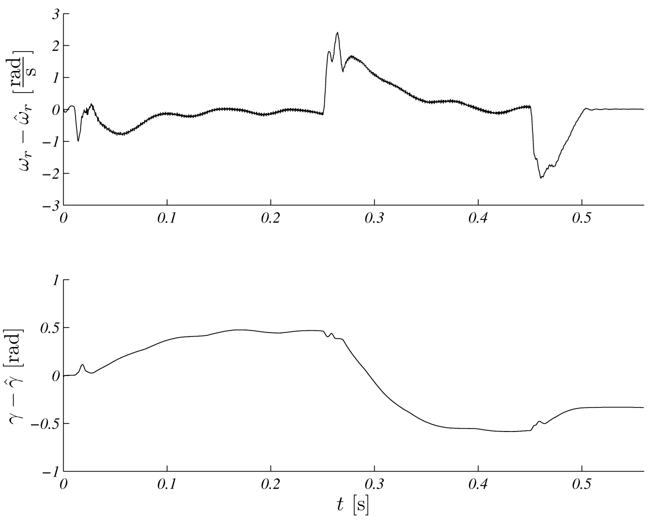

Fig. 12. UKF: reference speed $\omega_r^* = 5.28\ \frac{\mathrm{rad}}{\mathrm{s}}$ – estimation errors

Load torque. The idea of loading was presented in Subsec. "Load torque". The results of working are presented in Fig. 13. Each investigation was performed in the same way, the first non zero startup state vector during zero real speed, but the differences are additional load torque values.

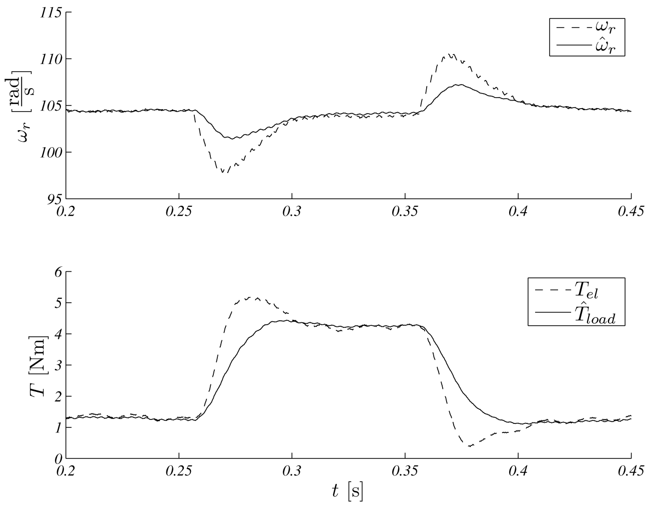

Fig. 13. UKF: load torque $T_l = 3\,\mathrm{Nm}$ response

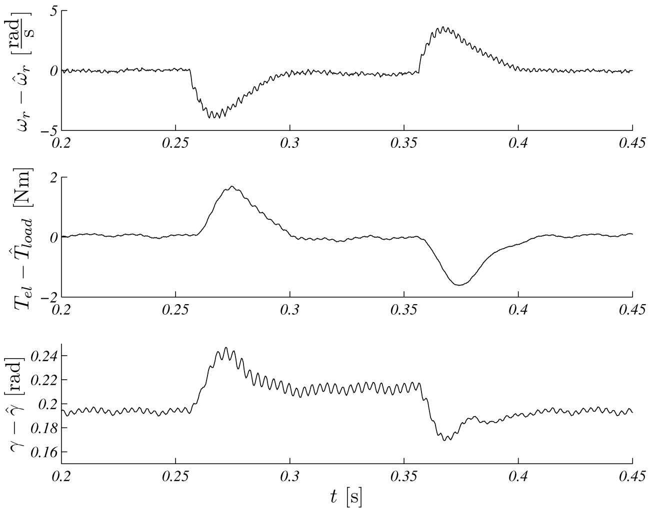

Fig. 14. UKF: load torque $T_l = 3\,\mathrm{Nm}$ response – estimation errors

From this investigation it can be concluded that the system values are estimated consistently regardless of the load torque conditions. In the steady state, the error of the state estimation is not great. Its maximum values depend on the dynamics of the state changes. The avoidance of the principle of constancy of load torque causes the appearance of significant errors in dynamic states. These appeared errors can be eliminated by changing the sensitivity of the observer, but changing the sensitivity causes a gain in the system and output noises. So in the case of cancelling dynamical errors we can expect to strengthen the unknown disturbance, in most cases nonlinear.

To compare the practical properties, two figures are presented here: the first is the average estimation error ϵ (Fig. 15), and second is the maximum error in a speed steady state (Fig. 16) in relation to the motor speed ω_r. Both observers give good steady-state performance.

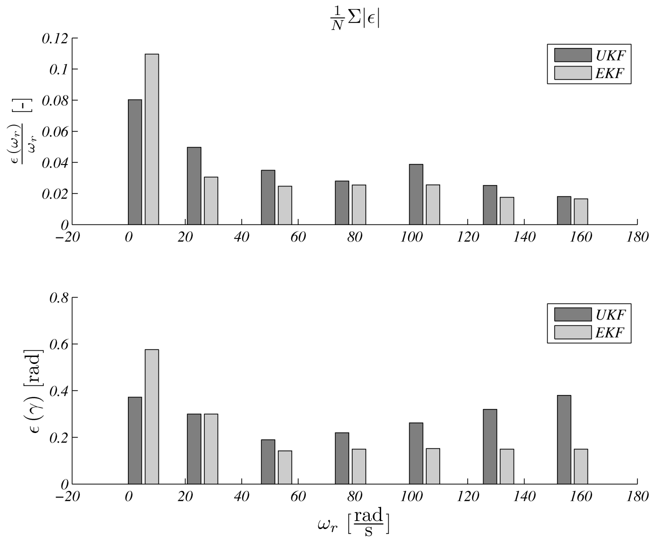

Fig. 15. Average estimation error of EKF and UKF

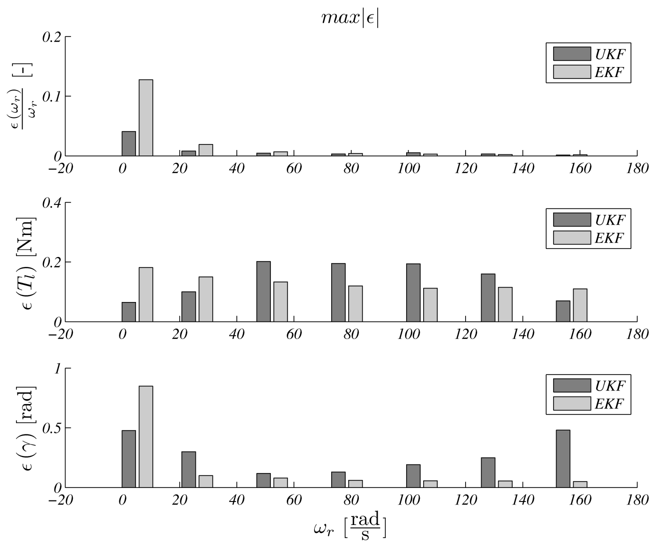

Fig. 16. Maximum of estimation error in speed steady state of EKF and UKF

Analysing the whole process of estimating the load torque and with those obtained from errors, it can be concluded that the observer reproduces all natural quantities of PMSM and disturbance as load torque is, with small trip-up.

5. Conclusions

The paper presents a design and laboratory verification of an observer based on two different Kalman filter techniques: the unscented Kalman filter and the extended Kalman filter. The state variable estimation of a non-linear object, which is a permanent magnet synchronous motor, was successfully accomplished. The estimated state variables were used as variables in a sub-cascade control system of currents and speed.

A control system with a UKF has better properties in the low speed range than the EKF. Also its starting procedure is safer, in that there are no situations with wrong starting direction. There are small errors during dynamical working caused by inaccurate modelling of the inverter, which is non-linear.

It can been seen during a start-up that the UKF performs better than the EKF. The drive is able to start from an unknown rotor position in all cases, unlike the EKF observer, where sometimes the speeds ω_r and $\widehat{\omega}_r$ directions are different. During the rush speed changes, for example reversing, UKF performs better, with smaller errors.

The unscented transformation approach has many advantages over the extended Kalman filter, namely, hassle-free tuning and finding the initial value. The UKF has an analytical derivative free structure and does not involves any linearisation steps–no Jacobian function is needed. But the EKF has a simpler matrix mathematical structure, so it was simpler to implement on DSP using special embedded matrix functions. UKF needs to calculate the sigma points during every time step. It may be noted based on compared execution times on DSP that the calculation time of UKF is larger than EKF.

REFERENCES

[1] S. Brock and K. Zawirski, "New approaches to selected problems of precise speed and position control of drives", *Proc. IECON 2012 – 38th Annual Conf. IEEE Industrial Electronics Society* 1, 6291–6296 (2012).

[2] M. Comanescu, "Rotor position estimation of pmsm by sliding mode emf observer under improper speed", *Industrial Electronics (ISIE), 2010 IEEE Int. Symp.* 1, 1474–1478 (2010).

[3] C. De Angelo, G. Bossio, J. Solsona, G. Garcia, and M. Valla, "Mechanical sensorless speed control of permanent-magnet ac motors driving an unknown load", *Industrial Electronics, IEEE Trans.* 53 (2), 406–414 (2006).

[4] R. Dhaouadi, N. Mohan, and L. Norum, "Design and implementation of an extended kalman filter for the state estimation of a permanent magnet synchronous motor", *Power Electronics, IEEE Trans.* 6 (3), 491–497 (1991).

[5] L. Grzesiak and M. Kazmierkowski, "Improving flux and speed estimators for sensorless ac drives", *Industrial Electronics Magazine, IEEE* 1 (3), 8–19, 2007.

[6] D. Janiszewski, "Load torque estimation in sensorless pmsm drive using unscented kalmana filter", *Industrial Electronics (ISIE), 2011 IEEE Int. Symp.* 1, 643–648 (2011).

[7] D. Janiszewski, "Unscented Kalman filter for sensorless pmsm drive with output filter fed by PWM converter", *Proc. IECON 2012 – 38th Annual Conf. IEEE Industrial Electronics Society* 1, 4660–4665 (2012).

[8] D. Janiszewski, "Load torque estimation for sensorless pmsm drive with output filter fed by pwm converter", *Proc. IECON 2013 – 39th Annual Conf. IEEE Industrial Electronics Society* 1, 1–6 (2013).

[9] S.J. Julier and J.K. Uhlmann, "A new extension of the kalman filter to nonlinear systems", *Int. Symp. Aerospace/Defense Sensing, Simul. and Controls, Proc.* 3, 12 (1997).

[10] S.J. Julier and J.K. Uhlmann, "Unscented filtering and nonlinear estimation", *Proce. IEEE* 92 (3), 401–422 (2004).

[11] T. Kaczorek, "Practical stability of positive fractional discrete-time linear systems", *Bull. Pol. Ac:. Tech.* 56 (4), 313–317 (2008).

[12] R.E. Kalman, "A new approach to linear filtering and prediction problems", *Trans. ASME – J. Basic Engineering* D 82, 35–45 (1960).

[13] M. Kazmierkowski, L. Franquelo, J. Rodriguez, M. Perez, and J. Leon, "High-performance motor drives", *Industrial Electronics Magazine, IEEE* 5 (3), 6–26 (2011).

[14] M.P. Kazmierkowski and H. Tunia, *Automatic Control of Converter-Fed Drives*, Elsevier Science & Technology, Amsterdam, 1994.

[15] J. Korbicz, M. Witczak, and V. Puig, "Lmi-based strategies for designing observers and unknown input observers for nonlinear discrete-time systems", *Bull. Pol. Ac:. Tech.* 55 (1), 1–42 (2007).

[16] R. Krishnan, J.D. Irwin, M.P. Kazmierkowski, and F. Blaabjerg, *Control in Power Electronics: Selected Problems*, Academic Press Series in Engineering, New York, 2002.

[17] A. Królikowski and D. Horla, "Robustness of adaptive discrete-time lqg control for first-order systems", *Bull. Pol. Ac:. Tech.* 58 (1), 89–97 (2010).

[18] M. Malinowski, M. Kazmierkowski, and A. Trzynadlowski, "A comparative study of control techniques for PWM rectifiers in ac adjustable speed drives", *Power Electronics, IEEE Trans.* 18 (6), 1390–1396 (2003).

[19] R. Muszynski and J. Deskur, "Damping of torsional vibrations in high-dynamic industrial drives", *Industrial Electronics, IEEE Trans.*, 57 (2), 544–552 (2010).

[20] T. Orłowska-Kowalska and M. Dybkowski, "Performance analysis of the sensorless adaptive sliding-mode neuro-fuzzy control of the induction motor drive with mras-type speed estimator", *Bull. Pol. Ac:. Tech.* 60 (1), 61–70 (2012).

[21] P. Pillay and R. Krishnan, "Modeling, simulation, and analysis of permanent-magnet motor drives. i. the permanent-magnet synchronous motor drive", *Industry Applications, IEEE Trans.* 25 (2), 265–273 (1989).

[22] Z. Qiao, T. Shi, Y. Wang, Y. Yan, C. Xia, and X. He, "New sliding mode observer for position sensorless control of permanent magnet synchronous motor", *Industrial Electronics, IEEE Trans.*, PP(99), 1 (2012).

[23] H. Rasmussen, "Sensorless speed control including zero speed of non salient pm synchronous drives", *Bull. Pol. Ac:. Tech.* 54 (3), 293–298 (2006).

[24] K. Shi, T. Chan, Y. Wong, and S. Ho, "Speed estimation of an induction motor drive using an optimized extended kalman filter", *Industrial Electronics, IEEE Trans.* 49 (1), 124–133 (2002).

[25] D. Simon, "Kalman filtering", *Embeded System Programming* 14 (6), 72–79 (2001).

[26] D. Simon, "Using nonlinear kalman filtering to estimate signals", *Embedded Systems Design* 19 (7), 38–53 (2006).

[27] K. Szabat and T. Orlowska-Kowalska, "Application of the kalman filters to the high-performance drive system with elastic coupling", *Industrial Electronics, IEEE Trans.* 59 (11), 4226–4235 (2012).

[28] K. Szabat, T. Orlowska-Kowalska, and K. Dyrcz, "Extended kalman filters in the control structure of two-mass drive system", *Bull. Pol. Ac:. Tech.* 54 (3), 315–325 (2006).

[29] K. Urbanski, "Sensorless control of pmsm high dynamic drive at low speed range", *Proc. IEEE Int Industrial Electronics (ISIE) Symp.* 1, 728–732 (2011).

[30] P. Vas, *Sensorless Vector and Direct Torque Control, Monographs in Electrical and Electronic Engineering* 42, Oxford University Press, Oxford, 1998.

[31] G. Zhu, L.-A. Dessaint, O. Akhrif, and A. Kaddouri, "Speed tracking control of a permanent-magnet synchronous motor with state and load torque observer", *Industrial Electronics, IEEE Trans.* 47 (2), 346–355 (2000).